

Article

# Influence of Phosphorus Addition on the Stress Rupture Properties of Direct Aged IN706 Superalloy

Sha Zhang <sup>1,\*</sup>, Anwen Zhang <sup>2</sup>, Chaochao Xue <sup>2</sup>, Dan Jia <sup>2</sup>, Weiwei Zhang <sup>2</sup>, Weiyang Wang <sup>3</sup>, Xin Xin <sup>2</sup> and Wenru Sun <sup>2</sup>

<sup>1</sup> College of Mechanical & Electrical Engineering, Changsha University, Changsha 410022, China

<sup>2</sup> Institute of Metal Research, Chinese Academy of Sciences, Shenyang 110016, China; awzhang13s@alum.imr.ac.cn (A.Z.); ccxue17s@imr.ac.cn (C.X.); djia@imr.ac.cn (D.J.); wwzhang16s@imr.ac.cn (W.Z.); xxin@imr.ac.cn (X.X.); wrsun@imr.ac.cn (W.S.)

<sup>3</sup> Jiangxi Province Key Laboratory of Polymer Preparation & Processing, Shangrao Normal University, Shangrao 334001, China; wang.weiyang.cmt@foxmail.com

\* Correspondence: szhang10b@alum.imr.ac.cn; Tel.: +86-731-8426-1492

Received: 19 June 2020; Accepted: 23 July 2020; Published: 24 July 2020



**Abstract:** This study investigated the influence of phosphorus (P) addition on the stress rupture properties of direct aged IN706 superalloy. The results showed that P slightly improved the stress rupture life of the superalloy when added in the range between 0.002% and 0.008%; however, it significantly reduced the stress rupture life when added in the range between 0.013% and 0.017%. Microstructure characterization indicated that the precipitation of  $\gamma'$ ,  $\gamma''$ , and  $\eta$  phases was not significantly affected by the addition of P. Phosphides precipitated in the alloy containing 0.017% P after aging at 980 °C for 10 min. Compared to a similar study previously made on IN706 superalloy, it was found that the optimum P concentration in the as-solutioned state for improving the stress rupture properties was not definite. Furthermore, the relationship between the amount of P segregated at the grain boundary and the role of P on the stress rupture properties was discussed.

**Keywords:** phosphorus; direct aging heat treatment; stress rupture property; grain boundary segregation; IN706 alloy

## 1. Introduction

Due to the increasing requirements on materials' thermal capabilities and on fuel efficiency, high temperature materials research has become more critical. Previous research has demonstrated that a minor addition of phosphorus (P) markedly improved the mechanical properties of some wrought Ni-Fe-based superalloys [1–10]. For example, P could increase the time to rupture more than 3-fold, and reduce the steady state creep by more than one order of magnitude in alloys such as IN718 and GH761, without obvious influence on tensile properties and grain size [1,2,11]. This leads to the development of superalloys with increased temperature capabilities without an increase in processing cost [12]. There have been several studies on the mechanisms behind the beneficial effects of minor P addition. These suggested that P tended to strongly segregate to grain boundaries, which enhances grain boundary strength [1,4,8,13], controls grain boundary precipitation [2–7,14,15], and inhibits intergranular oxidation [3].

In the past few decades, direct aging heat treatment has been widely used in the manufacture of gas turbine discs. Compared to solution annealing and aging heat treatment, direct aging efficiently achieves higher strength and finer grains in wrought superalloys, such as IN718, IN625, and IN783 [16–22]. It was also reported that direct aging enables a 10% increase in yield strength while maintaining sufficient creep resistance in IN718 alloy [17]. The superior strength was attributed to higher dislocation densities, lower  $\delta$  phase volume fraction, and fine precipitates [16].

As mentioned above, P microalloying and direct aging have been widely used in wrought superalloys. However, the effect of P on direct aged wrought superalloy remains unclear. Moreover, the effect of P on fine-grained superalloys is not yet fully understood. The Ni-Fe based IN706 alloy has good temperature strength and excellent machinability [23,24]. Therefore, it has been widely used in large gas turbine components below 700 °C [25,26]. In our previous work, the beneficial influence of P addition on stress rupture properties was confirmed in IN706 alloys under standard and nonstandard heat treatments [8]. Furthermore, it was found that P in the as-solutioned state improved the stress rupture properties, which was assumed to be the result of grain boundary strengthening.

In this work, IN706 alloys containing different P content were investigated to evaluate the influence of P on the microstructure and stress rupture properties of the direct aged alloy. Furthermore, the influence of P under direct aging, standard, and nonstandard schemes in IN706 alloy is summarized. The relationship between the level of P segregation at the grain boundaries and the role of P on stress rupture properties is discussed.

## 2. Materials and Methods

Experimental ingots were produced in a vacuum induction melting (VIM) furnace. To obtain an identical content of elements other than P, a master alloy was prepared. The composition of the master alloy was Fe-42.4, Ni-15.92, Cr-2.82, Nb-1.89, Ti-0.35, Al-0.0045, and B-0.04 C (wt.%). Subsequently, the master ingot was cut and remelted to make four 10 kg ingots with 90 mm diameter, to which four different P concentrations were added. The actual P contents of the four alloys were measured to be 0.002% (alloy 1), 0.008% (alloy 2), 0.013% (alloy 3), and 0.017% (alloy 4), respectively. All of the ingots were forged into bars of 35 mm × 35 mm cross section after being homogenized at 1160 °C for 20 h and then at 1190 °C for 40 h and cooled in air, and rolled into bars of 16 mm in diameter. The four rolled bars with different P contents were subjected to direct aging heat treatment: 730 °C for 8 h followed by cooling at 55 °C/h in a muffle furnace to 620 °C, then held at 620 °C for 8 h, and subsequently cooled in air. In addition, to investigate the distribution of P in the alloys, a sample of alloy 4 after direct aging heat treatment was held at 980 °C for 10 min and then water quenched.

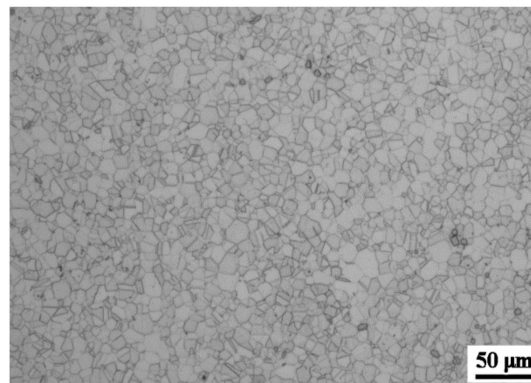
The stress rupture properties of direct aged IN706 alloys were tested at 650 °C and 690 MPa. Two samples were measured for each alloy. The HV microhardness was tested at room temperature under a load of 50 g for 15 s. The microhardness values used were an average of five measurements per sample, and all the microhardness values were measured in different grains.

The microstructures were characterized using FEI QUANTA 540 scanning electron microscopy (SEM) (FEI, Hillsboro, USA) and HITACHI SU8010 field emission SEM (HITACHI, Tokyo, Japan). The observations of the fracture surfaces after stress rupture testing were carried out using Hitachi S-3400 SEM (HITACHI, Tokyo, Japan). The phases at grain boundaries and in grain interiors were mainly determined using JEM-2100 transmission electron microscopy (TEM) (JEOL, Tokyo, Japan). The detailed process of sample preparation was reported elsewhere [8].

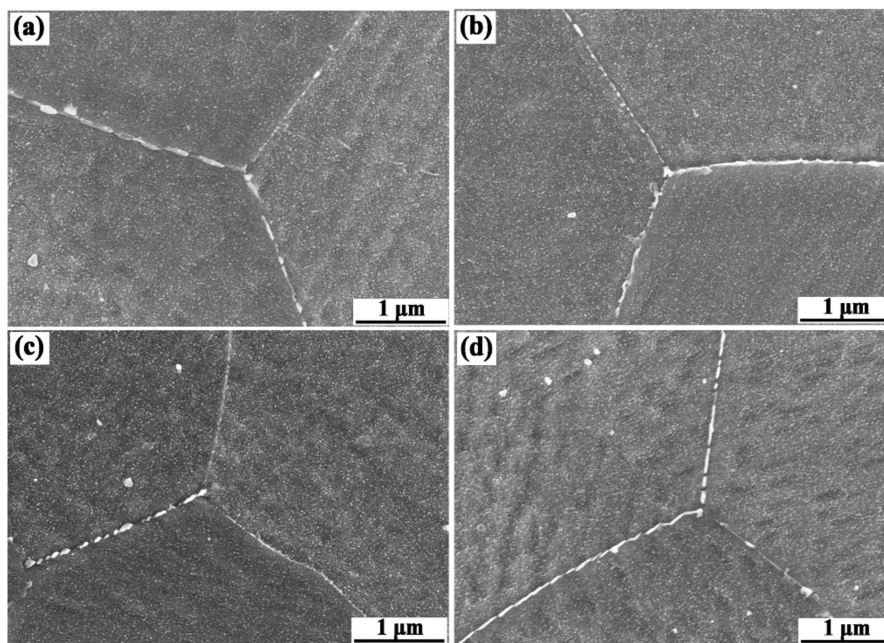
## 3. Results

### 3.1. Microstructure

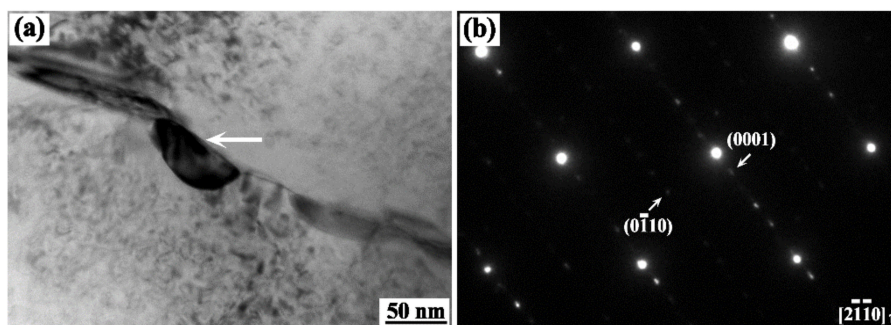
The average grain size for the direct aged alloys with four individual P contents was approximately 12 µm. Figure 1 shows the grain structure of alloy 3 as an example. SEM images of the alloys with four individual P contents are shown in Figure 2. The intergranular precipitates in the four alloys all appeared as short rod-like or granular particles. This observation indicates that P exerted no discernible influence on the precipitation of grain boundary phases. Figure 3 shows the TEM image and the corresponding selected area electron diffraction (SAED) pattern of grain boundary precipitate in alloy 4. The precipitates at grain boundaries were confirmed as η phase, which is the grain boundary-strengthening phase in IN706 superalloy.



**Figure 1.** Grain structure of alloy 3 after direct aging heat treatment.

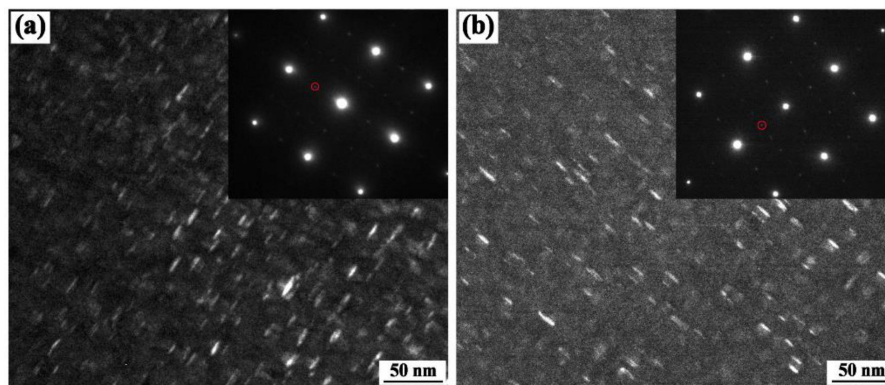


**Figure 2.** The microstructure of the alloys after direct aging heat treatment: (a) alloy 1, (b) alloy 2, (c) alloy 3, and (d) alloy 4.



**Figure 3.** (a) Bright-field TEM image and (b) the corresponding selected area electron diffraction (SAED) pattern of the precipitate at the grain boundary in alloy 4 after direct aging heat treatment.

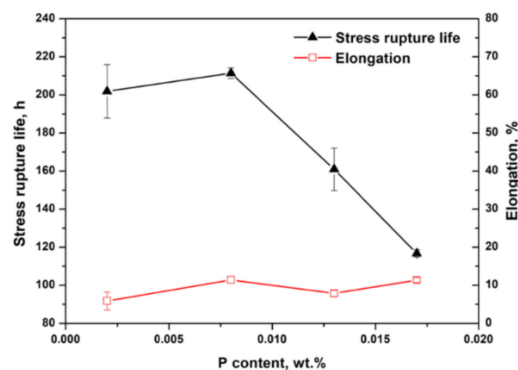
Figure 4 shows the precipitation of  $\gamma'$  and  $\gamma''$  phases in alloy 1 and alloy 4, respectively, after direct aging heat treatment. The corresponding SAED pattern is shown in the inset. Fine  $\gamma'$  and  $\gamma''$  phases can be seen in the interior of the grains. Morphology and distribution of the precipitates of alloy 1 and alloy 2 were similar; thus, they are not presented here. It was found that P addition did not obviously affect the precipitation of  $\gamma'$  and  $\gamma''$  phases.



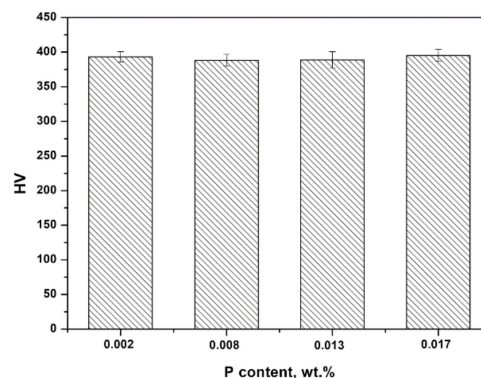
**Figure 4.** Dark-field TEM images and the corresponding SAED pattern in [001] zone axis: (a) alloy 1 and (b) alloy 4, imaged using (100) reflection.

### 3.2. Mechanical Properties

Figure 5 shows the stress rupture properties of direct aged alloys with four individual P contents. P slightly increased the time to rupture from 202 h to 211 h in the range of 0.002% to 0.008%, but it significantly decreased the stress rupture life in the range of 0.013% and 0.017%. In addition, the stress rupture elongation was not significantly affected by the P addition. Figure 6 shows the HV microhardness tested in the interior of grains in the alloy samples. It can be seen that the microhardness was not significantly influenced by P addition.



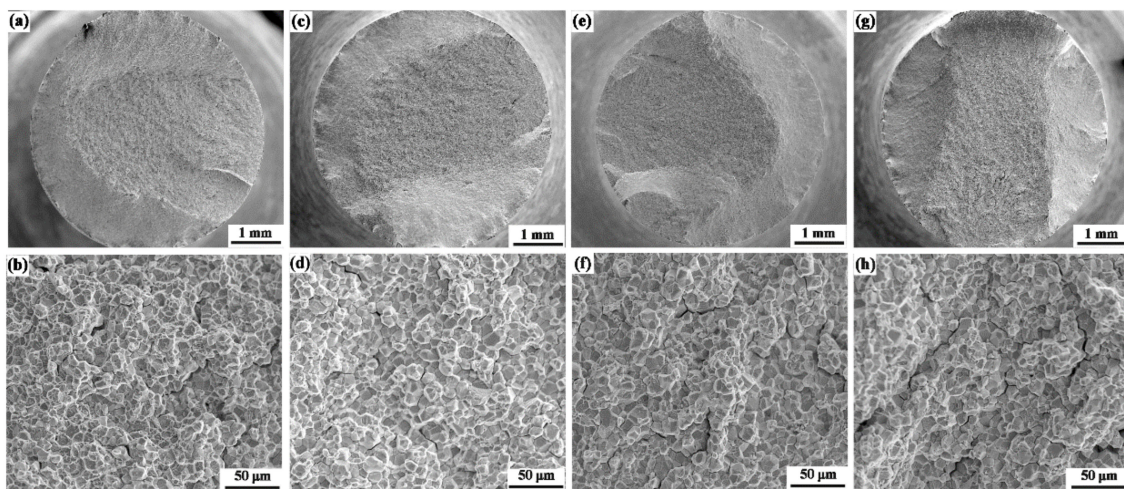
**Figure 5.** The stress rupture property of direct aged IN706 alloy with different P contents ruptured at 650 °C/690 MPa.



**Figure 6.** Microhardness of direct aged IN706 alloy with different P contents.

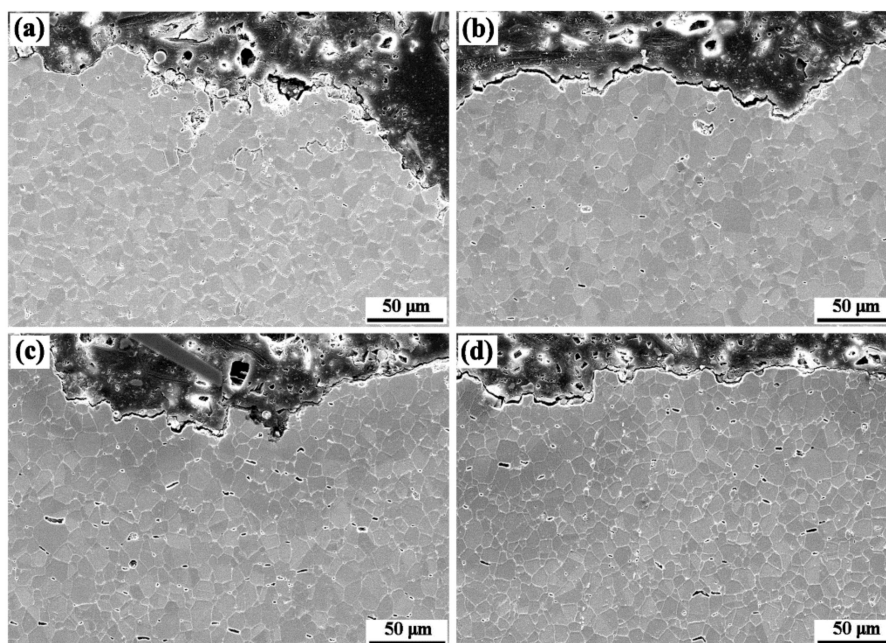
Figure 7 shows the morphology of the fracture surface of alloys after stress rupture testing. Both intergranular and transgranular fractured areas can be seen in the fracture surfaces of the four alloys [27]. Moreover, there were some secondary cracks on the intergranular fractured area, as shown in

Figure 7b,d,f,h. It is reasonable to speculate that the cracks originated at the grain boundaries. With the propagation of the intergranular cracks, the samples of alloys were eventually transgranular-fractured.



**Figure 7.** SEM images of the stress rupture fracture surface: (a,b) alloy 1, (c,d) alloy 2, (e,f) alloy 3, and (g,h) alloy 4. (b,d,f,h) show the enlarged views of the intergranular fracture area in corresponding alloys.

Figure 8 shows the microstructures of a longitudinal section near the fracture surface of the rupture samples. It was observed that a small number of intergranular cracks existed in the sample of alloy 1 and alloy 2. However, the number and size of intergranular cracks significantly increased in the sample of alloy 3 and alloy 4. The intergranular cracks indicate that the initiation of cracks first occurred at the grain boundaries.



**Figure 8.** SEM micrographs of longitudinal sections ruptured at 650 °C/690 MPa: (a) alloy 1, (b) alloy 2, (c) alloy 3, and (d) alloy 4.

#### 4. Discussion

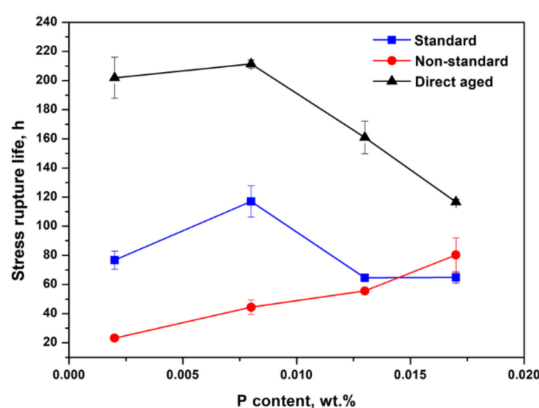
The addition of P on the stress rupture properties of IN706 alloy under the two different heat treatment schemes was studied in our previous work [8]. To outline the experimental results in the previous and present work, the heat treatment schemes and influence of P are shown in Table 1 and

Figure 9, respectively. It can be summarized as follows: (1) For the standard heat treatment scheme, P remarkably increased the stress rupture life when added within 0.002% to 0.008%. However, the stress rupture life dropped significantly when the P content was further increased to 0.013% and 0.017%, which corresponds to the precipitation of phosphide. (2) For the nonstandard heat treatment scheme, P always improved the stress rupture life when added between 0.002% and 0.017%. It should be noted that no phosphide precipitated in the alloys under this heat treatment scheme. (3) For the direct aging heat treatment scheme, P slightly increased the stress rupture life when added within 0.002% to 0.008%, but further addition of P resulted in a significant decrease of the stress rupture life. No phosphide was observed in the present work.

**Table 1.** Heat treatment schemes of IN706 alloy.

No.	Designation	Heat Treatment Cycle
1	Standard heat treatment	980 °C/3 h/AC + 845 °C/3 h/AC + 720 °C/8 h/furnace cooling at 50 °C/h to 620 °C + 620 °C/8 h/AC
2	Nonstandard heat treatment	1060 °C/2 h/AC + 720 °C/8 h/furnace cooling at 50 °C/h to 620 °C + 620 °C/8 h/AC
3	Direct aged heat treatment	720 °C/8 h/furnace cooling at 50 °C/h to 620 °C + 620 °C/8 h/AC

AC stands for air cooling.



**Figure 9.** Time to rupture IN706 alloy with different P content under three heat treatment schemes. The samples with standard and direct aged schemes were tested at 650 °C/690 MPa. The samples with nonstandard scheme were tested at 650 °C/650 MPa [8].

It was determined that P in the as-solutioned state is beneficial for the stress rupture properties by comparing the data obtained under the standard and nonstandard heat treatment schemes. It was previously suggested that the main mechanism of the beneficial effect of P addition is that moderate amounts of P in the as-solutioned state segregated to the grain boundaries, which increased grain boundary cohesion; reduced grain boundary free energy and diffusivity, which also served to prevent intergranular oxidation; and controlled the precipitation of the grain boundary phase [1–9,11]. However, P in the as-solutioned state was not always beneficial when the alloy was subjected to direct aging heat treatment, as shown in Figure 5. A possible reason for this divergent trend is discussed herewith.

It is widely accepted that the level of P grain boundary segregation strongly depends on the P content in the as-solutioned state and the heat treatment parameters [28,29]. The heat treatment schemes in the present work are different from those in the previous work [8], as the solution annealing step between the rolling and the aging steps is omitted for the direct aging heat treatment. As a result, the amount of P dissolved in the  $\gamma$  matrix is less because of the lack of solution treatment. Therefore,

it is inferred that direct aging heat treatment induced a higher segregation level of P at the grain boundaries than the heat-treatment schemes in the previous work [8].

To investigate P grain boundary segregation in the alloys, the direct aged alloy 4 was held at 980 °C for 10 min and subsequently water-quenched. The microstructure is presented in Figure 10. A number of phosphide particles precipitated at the grain boundaries. A study on Auger electron spectroscopy characterization has shown that P strongly segregates to the grain boundaries of IN706 alloy [30]. It is deduced that a small number of P atoms segregated at the grain boundaries of the direct aged alloy. As a result, the phosphide quickly precipitated at the grain boundaries during soaking at 980 °C, as shown in Figure 10. Liu et al. reported that excess P content could lead to a thin and fragile zone at the grain boundary, due to the repulsion between P atoms [31]. Sun et al. demonstrated that excess P segregation at grain boundaries deteriorated the grain boundary strength, leading to the reduction of the stress rupture life of IN718 alloy [3]. Thus, in the present work, we conclude that the excess P segregated at the grain boundaries of IN706 alloy is the main reason for the decrease of stress rupture life as P content exceeds 0.008%.

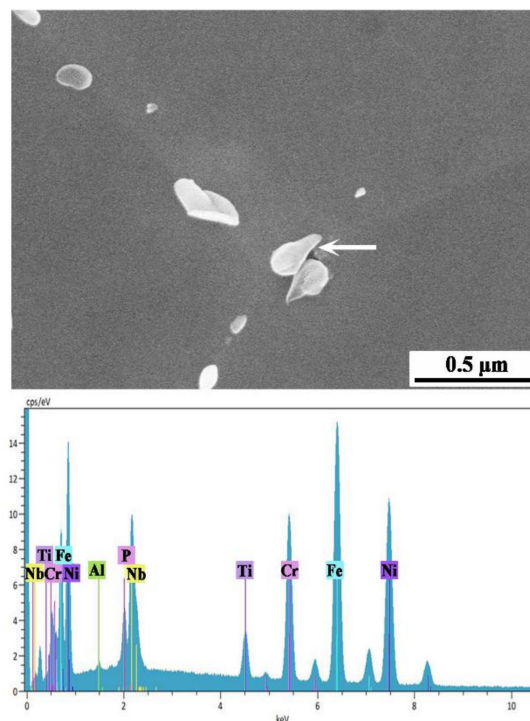


**Figure 10.** SEM image and EDS of the phosphide in alloy 4 held at 980 °C for 10 min after direct aging heat treatment.

From the above, we conclude that the influence of P in the as-solutioned state on the stress rupture properties of IN706 alloy is not definite. The optimum P concentration may depend on the level of P grain boundary segregation, which is influenced by factors such as P content, heat treatment temperature and holding time, and cooling rate. Therefore, to improve the property of wrought superalloys by manipulating P grain boundary segregation, the level of addition of P and thermal processing parameters should be comprehensively considered.

## 5. Conclusions

The aim of the present work was to investigate the influence of P addition on the microstructure and stress rupture properties of direct aged IN706 superalloy. Furthermore, the results were compared with our previous work. The main conclusions are as follows:

- (1) P slightly improved the stress rupture life when added in the range between 0.002% and 0.008%, but it significantly decreased the stress rupture life when added in the range between 0.013% and 0.017%. The precipitation of  $\gamma'$ ,  $\gamma''$ , and  $\eta$  phases was not significantly affected by P addition.
- (2) The beneficial effect of P could be primarily due to moderate amounts of P atoms segregated at the grain boundaries, which improved the cohesion of grain boundaries. However, excess P atoms at the grain boundaries could decrease the grain boundary cohesion, and thus deteriorate the stress rupture properties.
- (3) The optimum P in the as-solutioned state for the stress rupture properties was not definite. It may depend on the level of P grain boundary segregation, which was influenced by the P content and the heat treatment process.

**Author Contributions:** Conceptualization, S.Z.; methodology, A.Z.; validation, D.J.; formal analysis, A.Z.; investigation, C.X. and W.Z.; resources, W.S.; data curation, S.Z.; writing—original draft preparation, S.Z.; writing—review and editing, D.J.; visualization, C.X.; supervision, W.S.; project administration, X.X.; funding acquisition, S.Z. and W.W. All authors have read and agreed to the published version of the manuscript.

**Funding:** This work was funded by the Natural Science Foundation of Hunan Province of China (2020JJ4645), the Science Research Foundation of Hunan Provincial Education Department of China (grant number 19C0156), the Science and Technology Research Foundation of Jiangxi Provincial Education Department of China (grant numbers GJJ170929 and GJJ180868), and the National Natural Science Foundation of China (grant number 11964029).

**Conflicts of Interest:** The authors declare no conflict of interest.

## References

1. Cao, W.D.; Kennedy, R.L. The effect of phosphorous on mechanical properties of alloy 718. In *Superalloys 718, 625, 706 and Various Derivatives*; TMS: Warrendale, PA, USA, 1994; pp. 463–477.
2. Sun, W.R.; Guo, S.R.; Lu, D.Z.; Hu, Z.Q. Effect of phosphorus on the microstructure and stress rupture properties in an Fe-Ni-Cr base superalloy. *Metall. Mater. Trans. A* **1997**, *28*, 649–654. [[CrossRef](#)]
3. Sun, W.R.; Guo, S.R.; Lee, J.H.; Park, N.K.; Yoo, Y.S.; Choe, S.J.; Hu, Z.Q. Effects of phosphorus on the  $\delta$ -Ni<sub>3</sub>Nb phase precipitation and the stress rupture properties in alloy 718. *Mater. Sci. Eng. A* **1998**, *247*, 173–179. [[CrossRef](#)]
4. Guan, S.; Cui, C.Y.; Yuan, Y.; Gu, Y.F. The role of phosphorus in a newly developed Ni-Fe-Cr-based wrought superalloy. *Mater. Sci. Eng. A* **2016**, *662*, 275–282. [[CrossRef](#)]
5. Wang, M.Q.; Du, J.H.; Deng, Q.; Tian, Z.L.; Zhu, J. The effect of phosphorus on the microstructure and mechanical properties of ATI 718Plus alloy. *Mater. Sci. Eng. A* **2015**, *626*, 382–389. [[CrossRef](#)]
6. Hasebe, Y.; Yoshida, M.; Maeda, E.; Ohsaki, S. Effects of phosphorus addition on creep properties of wrought strengthened Ni-based superalloy. In *Proceedings of the 9th International Symposium on Superalloy 718 and Derivatives*; TMS: Warrendale PA, USA, 2018; pp. 527–540.
7. Wang, C.S.; Zhao, H.Q.; Guo, Y.A.; Guo, J.T.; Zhou, L.Z. Structural stability and mechanical properties of phosphorus modified Ni-Fe based superalloy GH984. *Mater. Res. Innov.* **2014**, *18*, 324–330. [[CrossRef](#)]
8. Zhang, S.; Zhang, A.W.; Chang, L.T.; Wang, W.Y.; Xin, X.; Sun, W.R. Effect of phosphorus on the stress rupture properties of IN706 superalloy. *Mater. Sci. Eng. A* **2019**, *761*, 137981. [[CrossRef](#)]
9. Wang, C.S.; Guo, Y.A.; Guo, J.T.; Zhou, L.Z. Investigation and improvement on structural stability and stress rupture properties of a Ni-Fe based alloy. *Mater. Des.* **2015**, *88*, 790–798. [[CrossRef](#)]
10. Wu, Y.S.; Qin, X.Z.; Wang, C.S.; Zhou, L.Z. Influence of phosphorus on hot deformation microstructure of a Ni-Fe-Cr based alloy. *Mater. Sci. Eng. A* **2019**, *768*, 138454. [[CrossRef](#)]
11. Antonov, S.; Isheim, D.; Seidman, D.N.; Tin, S. Phosphorous behavior and its effect on secondary phase formation in high refractory content powder-processed Ni-based superalloys. *Materialia* **2019**, *7*, 10043. [[CrossRef](#)]
12. Chang, L.T.; Sun, W.R.; Cui, Y.Y.; Yang, R. Influences of hot-isostatic-pressing temperature on microstructure, tensile properties and tensile fracture mode of Inconel 718 powder compact. *Mater. Sci. Eng. A* **2014**, *599*, 186–195. [[CrossRef](#)]
13. Liu, X.B.; Dong, J.X.; Tang, B.; Hu, Y.H.; Xie, X.S. Investigation of the abnormal effects of phosphorus on mechanical properties of INCONEL718 superalloy. *Mater. Sci. Eng. A* **1999**, *270*, 190–196. [[CrossRef](#)]

14. Hasebe, Y.; Takasawa, K.; Ohkawa, T.; Maeda, E.; Hatano, T. Grain boundary precipitation strengthening of phosphorus-added nickel-iron based superalloy. *Superalloys* **2016**, *2016*, 65–73.
15. Antonov, S.; Chen, W.; Lu, S.; Isheim, D.; Seidman, D.N.; Feng, Q.; Sun, E.; Tin, S. The effect of phosphorus on the formation of grain boundary laves phase in high-refractory content Ni-based superalloys. *Scr. Mater.* **2019**, *161*, 44–48. [[CrossRef](#)]
16. Theska, F.; Stanojevic, A.; Oberwinkler, B.; Ringer, S.P.; Primig, S. On conventional versus direct ageing of Alloy 718. *Acta Mater.* **2018**, *156*, 116–124. [[CrossRef](#)]
17. Krueger, D.D. The development of direct age 718 for gas turbine engine disk applications. In *Superalloys 718 Metallurgy and Applications*; TMS: Warrendale, PA, USA, 1989; pp. 279–296.
18. Krishna, S.C.; Gangwar, N.K.; Jha, A.K.; Pant, B.; Venkitakrishnan, P.V. On the direct aging of iron based superalloy hot rolled plates. *Mater. Sci. Eng. A* **2015**, *648*, 274–279. [[CrossRef](#)]
19. Theska, F.; Stanojevic, A.; Oberwinkler, B.; Primig, S. Microstructure-property relationships in directly aged Alloy 718 turbine disks. *Mater. Sci. Eng. A* **2020**, *776*, 138967. [[CrossRef](#)]
20. Enrique, P.D.; Jiao, Z.; Zhou, N.Y. Effect of direct aging on heat-affected zone and tensile properties of electrospark-deposited alloy 718. *Metall. Mater. Trans. A* **2019**, *50A*, 285–294. [[CrossRef](#)]
21. Burke, M.G.; Mills, W.J.; Bajaj, R. Microstructure and properties of direct-aged Alloy 625. In *Superalloys 718, 625, 706 and Various Derivatives*; TMS: Warrendale, PA, USA, 2001; pp. 389–398.
22. Ma, L.Z.; Chang, K.M.; Mannan, S.K.; Patel, S.J. Effect of thermomechanical processing of fatigue crack propagation in Inconel Alloy 783. In *Superalloys 2000*; TMS: Warrendale, PA, USA, 2000; pp. 601–608.
23. Schilke, P.W.; Pepe, J.J.; Schwant, R.C. Alloy 706 metallurgy and turbine wheel application. In *Superalloys 718, 625, 706 and Various Derivatives*; TMS: Warrendale, PA, USA, 1994; pp. 1–12.
24. Fesland, J.P.; Petit, P. Manufacturing alloy 706 forgings. In *Superalloys 718, 625, 706 and Various Derivatives*; TMS: Warrendale, PA, USA, 1994; pp. 229–238.
25. Kindrachuk, V.; Wanderka, N.; Banhart, J.; Mukherji, D.; Del Genovese, D.; Rösler, J. Effect of rhenium addition on the microstructure of the superalloy Inconel 706. *Acta Mater.* **2008**, *56*, 1609–1618. [[CrossRef](#)]
26. Mukherji, D.; Gilles, R.; Barbier, B.; Del Genovese, D.; Hasse, B.; Strunz, P.; Wroblewski, T.; Fuess, H.; Rösler, J. Lattice misfit measurement in Inconel 706 containing coherent  $\gamma'$  and  $\gamma''$  precipitates. *Scr. Mater.* **2003**, *48*, 333–339. [[CrossRef](#)]
27. Qiao, Y.X.; Tian, Z.H.; Cai, X.; Chen, J.; Wang, Y.X.; Song, Q.N.; Li, H.B. Cavitation erosion behaviors of a nickel-free high-nitrogen stainless steel. *Tribol. Lett.* **2019**, *67*, 1. [[CrossRef](#)]
28. Lejcek, P. *Grain Boundary Segregation in Metals*; Springer: Berlin, Germany, 2010; pp. 103–152.
29. Xu, T.D.; Cheng, B.Y. Kinetic of non-equilibrium grain-boundary segregation. *Prog. Mater. Sci.* **2004**, *49*, 109–208. [[CrossRef](#)]
30. Zhang, S.; Xin, X.; Yu, L.X.; Zhang, A.W.; Sun, W.R.; Sun, X.F. Effect of phosphorus on the grain boundary cohesion and  $\gamma'$  precipitation in IN706 alloy. *Metall. Mater. Trans. A* **2016**, *47*, 4092–4103. [[CrossRef](#)]
31. Liu, W.G.; Ren, C.L.; Han, H.; Tan, J.; Zou, Y.; Zhou, X.T.; Huai, P.; Xu, H.J. First-principles study of the effect of phosphorus on nickel grain boundary. *J. Appl. Phys.* **2014**, *115*, 043706. [[CrossRef](#)]

